Lees-Edwards boundary conditions for lattice Boltzmann suspension simulations

Eric Lorenz* and Alfons G. Hoekstra†
Section Computational Science, Faculty of Science, University of Amsterdam, Kruislaan 403, 1098 SJ Amsterdam

Alfonso Caiazzo§
INRIA Rocquencourt, Boîte Postale 105, F-78153 Le Chesnay Cedex, France
(Received 14 December 2008; published 26 March 2009)

When sheared suspensions are simulated, Lees-Edwards boundary conditions allow more realistic computational setups as they remove the need of a domain bounded by shearing walls (as in Couette-type flow) which bias typical flow structures. Lees-Edwards boundary conditions therefore allow investigation of pure bulk properties in a quasi-infinite system. In addition, they improve the computational efficiency of the simulations as the whole domain can be used to calculate averages. We propose an implementation of Lees-Edwards boundary conditions for lattice Boltzmann simulations of particulate suspensions, combined with an accurate treatment of fluid-particle interactions. The algorithm is validated using a simple single-particle benchmark and further applied to a fully resolved suspension flow. Shear-thickening behavior, which is prolonged to higher shear rates as compared to Couette flow results, could be observed.

DOI: 10.1103/PhysRevE.79.036706 PACS number(s): 02.70.−c, 47.57.E−, 47.11.Qr

I. INTRODUCTION

The dynamics of dense liquid-particle suspensions is of great importance for many physical, biological, and industrial processes. Suspension behavior is rich in rheological aspects triggered by various properties such as particle-fluid volume density, particle shape, size distribution, and properties of the suspending fluid [1]. The apparent viscosity ν_{app}, a crucial property describing a (complex) fluid at the macroscopic scale in general, depends on the shear rate $\dot{\gamma}$. Different types of viscosity behavior can be observed in a unitless parameter space described by the Reynolds number $\mathrm{Re}_p = 4\dot{\gamma}R^2/\nu_f$, expressing the ratio of inertial forces and viscous forces, and Péclet number $\mathrm{Pe}_p = 4\dot{\gamma}R^2/D$, the ratio of advection to diffusion (where $\dot{\gamma}R$ denotes a typical velocity, R the particle radius, ν_f the kinematic viscosity of the fluid, and D the diffusion coefficient). In general, from low to high Re_p and Pe_p a hard-sphere suspension shows the following behavior [2]: for small Re_p and Pe_p thermal fluctuations govern the system dynamics and lead to an increased viscosity due to the increased effective volume of the particles. Increase in the shear rate $\dot{\gamma}$ to mediate Re_p and Pe_p causes the viscosity to exhibit first shear thinning due to the decreasing influence of Brownian motion, followed by a Newtonian plateau where the particles of the suspensions are believed to be aligned in sheets parallel to the flow that are more easily sheared. Further increase in $\dot{\gamma}$ causes the suspension to thicken. Some experiments on real suspensions give rise to the assumption that this again is followed by a shear-thinning region [1].

Simulation approaches to address suspension rheology range from, in decreasing order of abstraction, (i) modeling the suspension as non-Newtonian fluid, (ii) continuum models of two-phase flows, and (iii) fully resolved particulate suspensions where the fluid dynamics is governed by the Navier-Stokes equations and the motion of the solid particles is governed by Newton's laws. In many practical problems, the more detailed level of description turns out to be necessary and Brownian motion has to be incorporated [3] for small particle sizes at small Reynolds numbers.

Lees-Edwards boundary conditions (LEBCs) [4] are routinely used in molecular dynamics (MD) simulations to maintain a constant shear over a periodically continued simulation box. They allow one to realize a sheared system without the need of explicit shearing solid walls.

Periodic boundary conditions are applied in the directions perpendicular to a shear velocity gradient while in the direction of the velocity gradient it is assumed that a copy of the system is moving with a velocity $\mathbf{u}_{\mathrm{LE}} = (u_{\mathrm{LE}}, 0)$ with respect to the original system and a velocity $\mathbf{u}_{\mathrm{LE}} = (-u_{\mathrm{LE}}, 0)$ on the opposite side. This induces a shear rate $\dot{\gamma} = u_{\mathrm{LE}}/L_y$ over the system height L_y.

The need to develop LEBCs for suspension simulations arises from the fact that the application of the common planar Couette viscometer scheme, where two moving parallel planar walls shear the fluid in between, gives results that are unavoidably affected by the presence of the walls. If we are interested in pure bulk properties we can use only a limited system fraction for measurements. Wall effects are the formation of a depletion zone near the wall and the resultant wall slip, both clearly observable in real suspensions [5,6] as well as in numerical simulations [7,8]. Suspended particles are limited in their mobility near the wall, leading to different particle structure and lower solid-fluid density near the wall resulting in a lower apparent viscosity in that region. Also, the wall slip decreases the shear rate over the bulk leading to a different situation than intended.

The use of the viscometer theme in lattice Boltzmann method (LBM) simulations has even greater impact. Here the fluid velocity is limited to low Mach numbers and viscosity has a lower bound to ensure stability of the relaxation scheme. This limits the system size at higher Re_p. Additionally, the system size itself is limited in lattice and particle

*e.lorenz@uva.nl
†a.g.hoekstra@uva.nl
§alfonso.caiazzo@inria.fr

size units to keep the problem computationally feasible. Therefore, with numerical simulations we cannot escape boundary effects. However, appropriate boundary conditions as proposed in this paper can minimize such effects.

In computational fluid dynamics formulations of LEBCs exist using other methods for particulate suspensions, for example a finite-element method together with a rigid-ring description of the particle [9]. For lattice Boltzmann methods LEBCs for suspensions in three dimensions (3D) [10] were reported but unfortunately no further details of the implementation were provided, nor answers to questions that arise when combining LEBCs with lattice-based models. In a recently published work [11], LEBCs were used to simulate deformable particles described by a finite-element method and coupled to LBM flow. In the present work we propose a method for a consistent coupling of Lees-Edwards boundary conditions with standard LBM suspension approaches (such as those by Ladd [12,13] or Aidun, Lu, and Ding [14–16]). In particular, we employ a corrected momentum exchange method (CMES), where S refers to suspensions the correction was originally developed for, together with a nonequilibrium refill method, both described in [17].

The lattice Boltzmann method is briefly introduced in Sec. II. In Sec. III, we discuss the implementation of LEBCs, while Sec. IV is dedicated to numerical tests. First, we validate the algorithms by a simulation of a single disk crossing a LE boundary. Then, we present simulations of a dense suspension and observe flow and particle density profiles as well as ν_{app} as a function of Re_p. Section V draws the conclusions.

II. LATTICE BOLTZMANN METHOD

The lattice Boltzmann method [18,19] an alternative approach to hydrodynamics offering a very efficient way to solve the discretized Boltzmann equation on regular lattices. The correct Navier-Stokes behavior can be approximated by proper choice of the equilibrium function.

We employ a two-relaxation-time (TRT) relaxation scheme [20], which offers a good balance between quality of results, computational cost, and implementation effort. It achieves a slight improvement in comparison to the lattice Bhatnagar-Gross-Krook (LBGK) scheme, the lattice implementation of the single-relaxation-time collision operator by Bhatnagar, Gross, and Krook [21] in terms of damping unphysical high-frequency modes, leading to more stable simulations at higher Pe_p.

At each time iteration t and at every node $\mathbf{r}$ of the lattice, we denote with $f_i=f_i(\mathbf{r},t)$ the particle densities traveling in directions of $\mathbf{e}_i$, where $\{i=1,\ldots,b\}$ denotes the discrete velocity space. During the *collision* step, these distributions are relaxed toward an equilibrium distribution f_i^{eq}. Unlike the LBGK method the TRT model uses two different relaxation times, and a collision operator can be defined as

$$\mathcal{C}(f_i)=\frac{1}{\tau}[f_i^{\mathrm{eq}}(f)-f_i]^{+}+\frac{1}{\tau_{-}}[f_i^{\mathrm{eq}}(f)-f_i]^{-}, \tag{1}$$

where F_i^{+} and F_i^{-} denote the even and the odd part, respectively, of a function on the discrete velocity space:

$$F_i^{+}=\frac{F_i+F_{i'}}{2},\quad F_i^{-}=\frac{F_i-F_{i'}}{2},$$

where i^* is such that $\mathbf{e}_{i'}=-\mathbf{e}_i$. Then, defining a propagation operator $\mathcal{P}$ the propagation step reads

$$\mathcal{P}f_i(\mathbf{r},t)=f_i(\mathbf{r}+\mathbf{e}_i,t+1). \tag{2}$$

The relaxation parameter τ is connected to the kinematic viscosity by $\nu=c_s^2(\tau-1/2)(\Delta x^2/\Delta t)$ [20,21] where c_s is the speed of sound. The equilibrium function is a function of the local velocity distribution through the density $\rho(f)$ and the velocity $\mathbf{u}(f)$, computed according to

$$\rho(\mathbf{r},t)=\sum_i f_i(\mathbf{r},t), \tag{3}$$

$$\rho(\mathbf{r},t)\mathbf{u}(\mathbf{r},t)=\sum_i \mathbf{e}_i f_i(\mathbf{r},t). \tag{4}$$

For ease of notation, in what follows, we will identify $f_i^{\mathrm{eq}}(\mathbf{f})=f_i^{\mathrm{eq}}(\rho(\mathbf{f}),\mathbf{u}(\mathbf{f}))$. Besides density and velocity, the momentum tensor can be computed as

$$\Pi_{\alpha\beta}(\mathbf{r},t)=\sum_i e_{i\alpha}e_{i\beta}f_i(\mathbf{r},t). \tag{5}$$

Conservation of mass, momentum, and kinetic energy are constraints to any equilibrium function $f_i^{\mathrm{eq}}(\mathbf{r},t)$ (and the Navier-Stokes equations for weakly compressible fluids are obtained [22]). Isotropy requires a multispeed model which involves at least nine lattice velocities $\mathbf{e}_i$ in 2D [22]. A suitable choice for f_i^{eq} for this model is

$$f_i^{\mathrm{eq}}=w_i\rho\left(1+\frac{1}{c_s^2}\mathbf{e}_i\cdot\mathbf{u}+\frac{1}{2c_s^4}(\mathbf{e}_i\cdot\mathbf{u})^2-\frac{1}{2c_2^2}u^2\right) \tag{6}$$

with the lattice velocities

$$\mathbf{e}_1=(1,0),\quad \mathbf{e}_2=(0,1),\quad \mathbf{e}_3=(-1,0),\quad \mathbf{e}_4=(0,-1),$$

$$\mathbf{e}_5=(1,1),\quad \mathbf{e}_6=(-1,1),\quad \mathbf{e}_7=(-1,-1),\quad \mathbf{e}_8=(1,-1),$$

and $\mathbf{e}_0=(0,0)$ for the rest particle distribution. The speed of sound is defined as $c_s=1/\sqrt{3}$ and the direction-dependent weights w_i read

	$i=0$	$i=1-4$	$i=5-8$
w_i	1/3	1/18	1/36

so that (6) agrees with an expansion of the Maxwell-Boltzmann distribution in small Mach numbers u/c_s to the order of u^2.

The LBM scheme can be written as

$$\mathcal{P}f_i(\mathbf{r},t)=\mathcal{C}f_i(\mathbf{r},t) \tag{7}$$

using propagation and collision operators defined in (2) and (1).

It can be shown that in the asymptotic limit, the stress tensor

$$S_{\alpha\beta}(\mathbf{r},t)=[\Pi_{\alpha\beta}(\mathbf{r},t)-\mathbf{C}(\mathbf{r},t)](\Delta x/\Delta t)^2 \tag{8}$$

and pressure $p=(\rho-\rho_0)c_s^2(\Delta x/\Delta t)^2$ can be obtained locally. Here, ρ_0 denotes a constant reference density which is typi-

cally set to 1 in simulations. In practice, $\Pi_{\alpha\beta}$ has to be calculated as the mean over precollision and postcollision densities f_i and $\mathcal{C}f_i$. $\mathbf{C}(\mathbf{r},t)=\rho(\mathbf{r},t)\mathbf{u}(\mathbf{r},t)\mathbf{u}(\mathbf{r},t)$ is the local convection tensor.

Throughout the remainder of this paper all quantities will be given in lattice units, setting $\Delta x=\Delta t=1$.

A. Direct simulation of suspended particles

To implement no-slip solid-fluid boundary conditions in the present work we used the bounceback at the links (BBL) method, assuming the boundary to be always located at the midpoint of boundary links (BL), i.e., of the lattice links that are cut by the solid-fluid interface. More sophisticated and accurate methods [23–25] exist and, in principle, can be combined with the ideas of the following sections. However, for clearness we stick here to the BBL description. In the case of BBL with moving solid surface, the propagation step is given by

$$\mathcal{P}f_i(\mathbf{r},t_+)=\begin{cases}\mathcal{R}_{\mathbf{u}_b}f_{i'}(\mathbf{r},t_+) & \text{if } i' \text{ is BL},\\ f_i(\mathbf{r}+\mathbf{e}_{i'},t_+) & \text{else},\end{cases} \tag{9}$$

using a reflection operator

$$\mathcal{R}_{\mathbf{u}_b}f_i=f_i+2w_ic_s^{-2}\mathbf{u}_b\cdot\mathbf{e}_i \tag{10}$$

where $\mathbf{u}_b$ is the velocity of the midpoint of the boundary link and i' denotes the opposite direction to i. If the fluid node is not virtual, an amount of momentum

$$\delta\mathbf{p}_i=2\mathbf{e}_{i'}[\mathcal{C}f_{i'}(\mathbf{r},t+1)-\rho w_i(c_s^{-2}\mathbf{u}_b\cdot\mathbf{e}_i+T_{\mathrm{CJ}})] \tag{11}$$

is transferred to the particle. T_{CJ} is a correction term. The transferred momentum $\delta\mathbf{p}_i$ gives rise to a force and a torque acting at the boundary point $\mathbf{r}_b=\mathbf{r}+\frac{1}{2}\mathbf{e}_{i'}$ according to

$$\mathbf{F}(\mathbf{r}_b,t+1/2)=\delta\mathbf{p}_i/\Delta t \tag{12}$$

$$\mathbf{T}(\mathbf{r}_b,t+1/2)=(\mathbf{r}_b-\mathbf{R})\times\mathbf{F}(\mathbf{r}_b,t+1/2), \tag{13}$$

where $\mathbf{R}$ is the center of mass of the particle.

The original momentum exchange algorithm (MEA) proposed by Ladd [12,13] is obtained by setting $T_{\mathrm{CJ}}=0$. However, the MEA produces strong shear- and velocity-dependent particle behavior in situations where the particle exceeds the original domain and is partly described in another reference frame (see also Fig. 2). As shown in [17,26] the correction term

$$T_{\mathrm{CJ}}=-c_s^{-4}(\mathbf{u}_b\cdot\mathbf{e}_i)^2+c_s^{-2}\mathbf{u}_b^2 \tag{14}$$

efficiently removes the leading order of non-Galilean effects. This correction term is the essential improvement proposed with the corrected momentum exchange for suspensions [17]. The violation of Galilean invariance by the MEA, when used *locally*, has been already observed in [27] and cured by the introduction of additional virtual fluid nodes inside the solid domain. However, this is a workaround and care has to be taken at the implementation of such an idea when boundary links cross a Lees-Edwards boundary. The correction (14) offers a consistent analytical solution and, in most cases, allows an easier implementation.

Another consequence of the lattice representation is that nodes are covered or uncovered while particles are moving. In the method by Aidun *et al.* (ALD) [14–16] the fluid momentum of such a node is given to or taken from the particle, respectively. Such an extra momentum exchange is not necessary in the suspension method by Ladd [12,13] where the inner fluid is physical and contributes to the particle dynamics. However, in both methods the inner fluid, whether virtual or physical, is used to spare the reinitialization of fluid nodes. It is assumed that the properties of an inner fluid already satisfies the outside boundary situation when it is uncovered. However, we could show [17] that this approach may lead to unphysical behavior when particles are following each other in the flow. An improved refill method was proposed in [28]. In [17] we successfully employed an efficient refill method based on the decomposed interpolation of equilibrium and nonequilibrium parts of the f_i's [29], which significantly improves the situation of two particles following each other, and removes the need to simulate inner fluid.

In situations where particles are near contact it happens that in the lattice representation no fluid node exists between the particles causing the lubrication to break down. In order to resolve this, either the grid needs to be refined appropriately or a model of lubrication forces based on theoretical lubrication approximation has to be used for correction. We applied a single-term two-particle lubrication force derived from linear lubrication theory for the force between two cylinders [8].

Using the net force and torque on the particle resulting from contributions of the momentum transfer during fluid reflection at boundary links and the lubrication forces the motion of the solid particle is determined by its Newtonian equations of motion and can be solved using a velocity-verlet scheme or, as in our case, a fourth-order Runge-Kutta integration to resolve the dynamics as correctly as possible with a given time step also in cases when particles are very close and therefore force gradients are very steep.

III. LEES-EDWARDS BOUNDARY CONDITIONS

It what follows we present a method for suspension simulations that allows the consistent treatment of solid particles crossing the boundary between systems which move respect to each other. It is an extension of the method by Wagner and Pagonabarraga for fluid-only lattice Boltzmann systems [30], where fluid densities that cross a LE boundary have to undergo two steps in addition to normal periodic propagation. The first problem is the implementation of a velocity shift in a method with a fixed set of velocities of densities instead of particles with real coordinates. A Galilean transform has to be applied to the distributions, $f_{i,\mathbf{u}_0}\rightarrow f_{i,\mathbf{u}_0\pm\mathbf{u}_{\mathrm{LE}}}$ where $\mathbf{u}_0$ denotes the reference velocity of the computational domain, and $\mathbf{u}_{\mathrm{LE}}=(u_{\mathrm{LE}},0)$ denotes the velocity shift between the system copies. Following [30] a transform rule can be derived from an approximation of (1),

$$f_i=f_i^{\mathrm{eq}}+\tau(\partial_t f_i^{\mathrm{eq}}+c\mathbf{e}_i\nabla f_i^{\mathrm{eq}})+O(\partial^2). \tag{15}$$

All terms of order $O(\partial)$ can be skipped, because their zeroth and first moments are of negligible order $O(\partial^3)$. The $\mathbf{u}$ de-

pendence is kept and one arrives at a rather simple expression for the change in the boundary-crossing density due to the transform, which reads

$$f_{i,\mathbf{u}_0+\mathbf{u}_{\mathrm{LE}}} - f_{i,\mathbf{u}_0} \approx f_i^{\mathrm{eq}}(\rho,\mathbf{u}+\mathbf{u}_{\mathrm{LE}}) - f_i^{\mathrm{eq}}(\rho,\mathbf{u}), \tag{16}$$

where $\rho=\rho(\mathbf{f}(\mathbf{r},t))$ and $\mathbf{u}=\mathbf{u}(\mathbf{f}(\mathbf{r},t))$. From that we define a Galilean transform operator

$$\mathcal{G}_{\mathbf{u}_{\mathrm{LE}}} f_i = f_i + f_i^{\mathrm{eq}}(\rho,\mathbf{u}+\mathbf{u}_{\mathrm{LE}}) - f_i^{\mathrm{eq}}(\rho,\mathbf{u}) \tag{17}$$

that has to be applied to all densities that cross a LEBC. The local density is conserved under this transform.

Another issue in defining a consistent LEBC for lattice Boltzmann systems is that the shift between the system copies s_{LE} does not necessarily correspond to an integer multiple of the lattice spacing. In practice, densities crossing a LE boundary have to be mapped to the destination lattice by an interpolation. More precisely, they have to be distributed over the two cells that partly overlap the virtual destination cell. For the simple case of only fluid nodes, for the propagation of densities that are fed from nodes in a shifted reference frame, we can write

$$\mathcal{P}_{\mathrm{LE}} f_i(\mathbf{r}) = s_1 \mathcal{G}_{\mathbf{u}_{\mathrm{LE}}} f_i(\mathbf{r}_1 - \mathbf{e}_i) + s_2 \mathcal{G}_{\mathbf{u}_{\mathrm{LE}}} f_i(\mathbf{r}_2 - \mathbf{e}_i) \tag{18}$$

with

$$s_1 = \mathrm{mod}(s_{\mathrm{LE}},1),$$

$$s_2 = 1 - \mathrm{mod}(s_{\mathrm{LE}},1), \tag{19}$$

$$\mathbf{r}_1 = (x + \mathrm{int}(s_{\mathrm{LE}}) + 1, y),$$

$$\mathbf{r}_2 = (x + \mathrm{int}(s_{\mathrm{LE}}), y). \tag{20}$$

Including solid-fluid interaction given by (9) for the propagation of densities that may cross a LE boundary we can write

$$\mathcal{P}_{\mathrm{LE}} f_i(\mathbf{r}) = s_1 \begin{cases} \mathcal{R}_{\mathbf{u}_b} f_{i'}(\mathbf{r}) & \text{if } L_1 \text{ is BL,} \\ \mathcal{G}_{\mathbf{u}_{\mathrm{LE}}} f_i(\mathbf{r}_1 - \mathbf{e}_i) & \text{else,} \end{cases} + s_2 \begin{cases} \mathcal{R}_{\mathbf{u}_b} f_{i'}(\mathbf{r}) & \text{if } L_2 \text{ is BL,} \\ \mathcal{G}_{\mathbf{u}_{\mathrm{LE}}} f_i(\mathbf{r}_2 - \mathbf{e}_i) & \text{else.} \end{cases} \tag{21}$$

This approach is motivated by subgrid-scale boundary conditions proposed by Verberg and Ladd [23]. There also, partially covered destination nodes caused a splitting of propagated densities.

To illustrate the application of the propagation operator $\mathcal{P}_{\mathrm{LE}}$ Fig. 1 depicts the fate of f_5 densities that propagation vectors point outside the original domain. Density $f_5(\mathbf{r}_{(1)})$ is split into two parts $s_1 f_5(\mathbf{r}_{(1)})$ and $s_2 f_5(\mathbf{r}_{(1)})$ which are propagated to the two nodes of the shifted copy that partly overlap the ghost node it would go to by the application of $\mathcal{P}$. On both parts the action of $\mathcal{G}_{\mathbf{u}_{\mathrm{LE}}}$ will be applied. In the case of $f_5(\mathbf{r}_{(2)})$ one part, $s_1 f_5(\mathbf{r}_{(1)})$, is reflected by the action of $\mathcal{R}_{\mathbf{u}_b'}$ because the corresponding destination node belongs to the particle. In this case, $\mathbf{u}_b$ is transformed to $\mathbf{u}_b'=\mathbf{u}_b+(u_{\mathrm{LE}},0)$ because the particle is described by its center residing in the reference frame moving with u_{LE} with respect to the original frame. In the case of $f_5(\mathbf{r}_{(3)})$ both parts are reflected by $\mathcal{R}_{\mathbf{u}_b'}$. For the case when the suspension model includes the description of the inner fluid, the density $f_5(\mathbf{r}_{(4)})$ undergoes a similar procedure as $f_5(\mathbf{r}_{(1)})$.

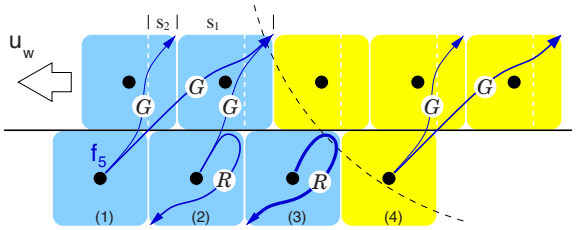

FIG. 1. (Color online) Illustration of the cases to be distinguished during the propagation of f_5 densities in a model case. Shown are some of the nodes of the upper boundary layer and a part of the lower layer at a Lees-Edwards boundary. Yellow (light gray) nodes belong to a particle crossing the boundary; blue (mid-gray) are fluid nodes. $\mathcal{G}$ denotes the application of the Galilean transform (17), $\mathcal{R}$ the application of the reflection operator (10).

IV. NUMERICAL RESULTS

A. One particle crossing LE boundary

As an essential validation of the implementation of LE boundary conditions we let a single particle cross the LE boundary. No external forces are applied to the particle. Using LEBCs where no solid objects are needed to drive the flow and therefore no preferred reference exists, we are able to superimpose the sheared flow with any constant velocity as long as actual lattice velocities are kept in a range where the LBM is valid.

In detail, we placed a particle at the midpoint of a squared domain, with an initial velocity equal to the fluid velocity at that point $\mathbf{v}_{\mathrm{p}}(t=0)=\mathbf{u}_s(t=0)=(0.025,0.005)$ which represents the velocity that is superimposed to a normal shear flow with the particle at its $\mathbf{v}_{f,x}=\mathbf{0}$ line. The flow is initialized and maintained at a horizontal shear $\dot{\gamma}=u_w/L_y=1.25\times10^{-5}$ and the particle's angular speed is set accordingly as $\omega(t=0)=\dot{\gamma}/2$. After a short equilibration time, the near-particle flow field is equilibrated and the particle moves freely along with the fluid and crosses the LE boundary. In Fig. 2 the y component of the particle speed is plotted as obtained by different suspension methods. Ideally, conserving Galilean invariance, the velocity should stay constant. However, deviations can be observed from the beginning for the ALD method. Ladd's method conserves the speed perfectly until the particles crosses the LE boundary. It turned out that this results from non-Galilean effects of the momentum exchange algorithm used in both cases [17]. In Ladd's case, as long as the particle resides completely in one reference frame, those effects are eliminated by the use of the inner fluid where the momentum exchange process between the outer fluid and the solid has its antiparallel counterpart in the inner fluid. This exactly eliminates any dependence on the superimposed velocity. To exploit this effect also for the ALD method in [11] physical nodes were added at the inner surface. However, in

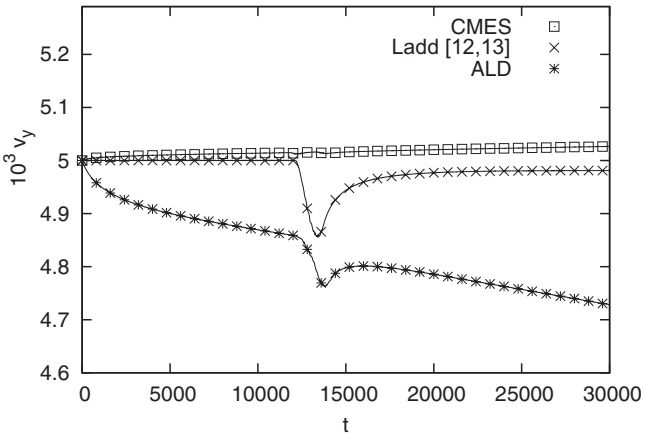

FIG. 2. y component of the particle's velocity $\mathbf{v}_{p,y}$ while the particle is freely moving at a $\mathbf{v}_{f,x}=0$ position of a shear flow with rate $\dot{\gamma}=1.25\times10^{-5}$. The whole system is superposed with a velocity $\mathbf{v}_s=(0.025,0.005)$, therefore expecting a constant $\mathbf{v}_{p,y}=0.005$. A systematic violation of Galilean invariance can be observed for the ALD method over the whole simulation time. During the period $t\approx12\,000-15\,000$, when the particle crosses the LE boundary, strong deviations can be observed for both methods not applying the correction to the MEA. The maximum Mach number did not exceed Ma=0.0487 in the course of the experiments.

the case the particle is partly described in one reference frame and the other part in another reference frame with a different underlying velocity, this correcting effect is absent. Using the corrected momentum exchange algorithm we were able to repeat the experiment obtaining satisfactory results (Fig. 2). Using CMES non-Galilean effects are minimized and the particle crosses the LE boundary practically unaffected. The remaining deviations can be related to discretization errors on the near-particle flow field, and do not affect the leading orders, relevant for the hydrodynamics. We could confirm this by simulations with successively increased grid resolution.

In conclusion, the results in Fig. 2 show that the proposed LEBC algorithm allows consistent simulations of suspensions, sheared according to the Lees-Edwards idea.

B. Suspension in sheared flow

Next, we simulate sheared suspensions with a solid-fluid fraction $\phi=0.40$ using the LEBC method and the Couette scheme for comparison of the flow fields. In a squared system of size $L_x\times L_y=259\times259$ lattice nodes, we suspended 133 particles with a radius $R_p=8.0$. The suspension was sheared at particle shear Reynolds numbers $\mathrm{Re}_p=0.005,0.2,1.0$ and profiles of velocity and the solid-fluid ratio were measured. Averages were obtained over a shear of $s_{\mathrm{LE}}=10L_x$.

Employing the Couette condition a clear deviation from the Newtonian velocity profile can be seen for $\mathrm{Re}_p\gtrsim0.1$, as shown in Fig. 3. Close to the walls an increasing slip becomes clearly detectable which lowers the velocity gradient over the bulk. This behavior could already be seen in simulations of hard-sphere suspensions [31] as well as experimental setups [6].

Figure 3 shows the plot of $\phi(y)$, demonstrating that the profile deviates from the linear Newtonian profile in two aspects.

(i) Especially close to the walls, particle densities oscillate with a period of slightly more than one particle width. This suggests that particles tend to align to the walls forming sheets [32]. Such structures of particles parallel to the shear velocity decrease the average interparticle friction.

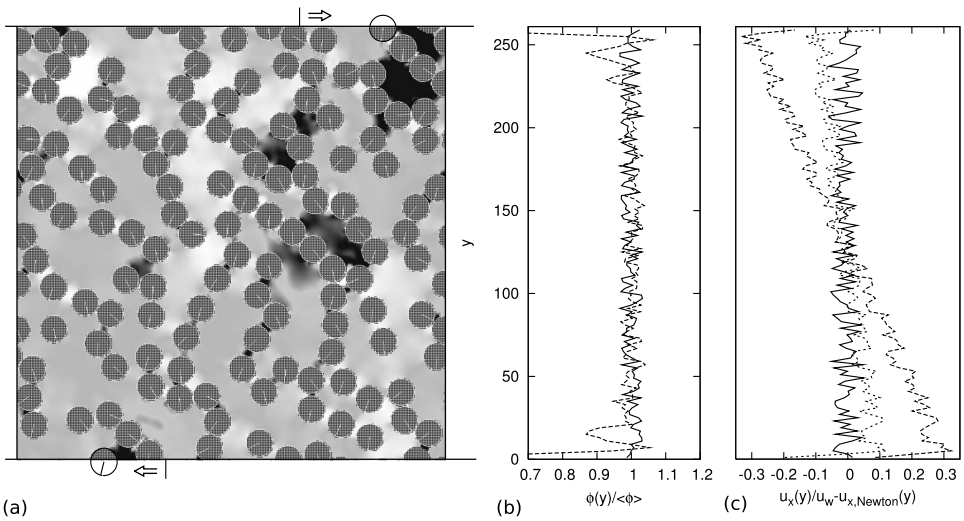

FIG. 3. (a) Snapshot of a sheared suspension of 133 disks of radius $R=8.0$ in a domain of 259×259 lattice sites. The particle-shear Reynolds number $\mathrm{Re}_p\approx1.5$. The grayscale code indicates low- (dark) and high-pressure (bright) areas. Note the typical particle and pressure field structures that would be inhibited by walls in a Couette scheme. (b), (c) Comparison of profiles as obtained by application of the Couette scheme (dotted line) and Lees-Edwards boundary conditions (solid line). (b) The local average particle density $\phi(y)$ shows strong wall effects in the Couette case. Using LEBCs particles are homogeneously distributed over the system height. Both profiles were measured at $\mathrm{Re}_p=1.0$. (c) The velocity profiles $v_x(y)$ as obtained using Couette boundary conditions show increasing slip effects near the wall for $\mathrm{Re}_p=0.1$, 1.0. Using LEBCs at $\mathrm{Re}_p=1.0$ no systematic deviations from the Newtonian profile can be seen.

(ii) The average particle density near the wall is less than in the bulk. The presence of the wall alone causes a lift force on the particles [33] and causes a depletion zone, according to observations in experimental setups [5]. Another effect of sheetlike structures of particles is that the mobility of particles is inhibited. Particles of sheets sliding along each other mostly collide with small collision cross sections, pushing the particles back into the sheet.

Both effects lower the viscosity and therefore lead to the observed wall slip.

Repeating the same experiments using LEBCs we obtain improved behavior. Here fluid and particles experience homogeneity. Particles are free to form configurations typical for a certain shear rate all over the domain. In fact, the plots of the profiles on the left of Fig. 3 show a flat distribution of particles over the system height and no systematic deviations from the Newtonian velocity profile.

C. Shear-thickening suspension

A highly relevant aspect of hard-sphere suspension rheology is shear thickening at higher particle shear Reynolds numbers Re_p. Already in the Stokes regime the existence of solid particles causes a higher apparent viscosity. The increase of the relative apparent viscosity with higher solid-fluid fractions ϕ is best described by the semiempirical Krieger-Dougherty relation [34]

$$\frac{\nu}{\nu_{\mathrm{f}}} = \left(1 - \frac{\phi}{\phi_{\max}}\right)^{-[\eta]\phi_{\max}} \tag{22}$$

where $\phi_{\max}=0.82$ is the solid-fluid fraction in 2D at which particles are packed densely enough that any particle flow is impeded and therefore the viscosity diverges. $[\eta]$ is an intrinsic viscosity of the suspension and equals 2 in 2D. It has been shown that the ALD and Ladd [12,13] methods can reproduce the Krieger-Dougherty relation in a convincing accuracy over the range of implementable fluid-solid ratios in the range of small Re [7,8]. In Fig. 4 we present measurements of the increase of ν_{app} over a wide range of solid-fluid ratios ϕ as obtained by CMES. The same system settings as for the simulations in the previous sections were used. The results agree well with the expected Krieger-Dougherty behavior.

For shear-thickening measurements we used a system with size 259×259 and 133 suspended disks with a radius of $R=8$, resulting in a solid-fluid ratio of $\phi=0.40$. The density ratio was set to $\rho_s/\rho_f=10$. We used the latter value to be able to give direct comparisons with the shear-thickening simulations presented in [8]. To obtain the apparent viscosity we followed the method presented in [7,31], which allows shear stresses to be measured in the bulk instead of measuring frictional forces at the walls. Shear stresses can be calculated along a horizontal plane as the sum over the contributions from the fluid and solid phase as outlined in [31]. We obtained stresses by averaging measurements over ten equally distributed planes and a shear of at least $10L_x$. In the case of Couette boundary conditions we took care that only bulk properties were measured by distributing the stress planes in such a manner that none of them was closer than 50 lattice sites to the wall. Looking at the profiles in Fig. 3 we can safely assume that direct influences of the walls are absent at this distance. Use of LEBC measurements can be carried out over the whole system height. This increases the bulk area we are interested in significantly.

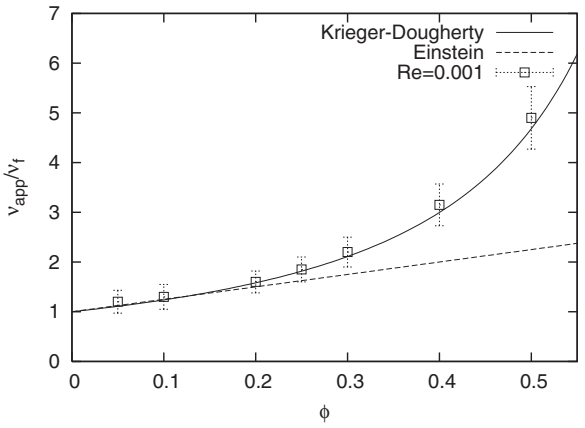

FIG. 4. Increase of the relative apparent viscosity ν_{app} as a function of the solid-fluid ratio ϕ for $\mathrm{Re}\ll 1$ as obtained by a simulation using CMES compared to the theoretical behavior proposed by the Krieger-Dougherty and Einstein approximations for small ϕ. A comparison between Couette and LEBC results shows no significant difference in this regime.

In Fig. 5 apparent viscosities are shown, normalized by the Krieger-Dougherty relation obtained for a range of Re_p from 0.001 to 4.0. The maximum achievable Reynolds number is limited by stability conditions of the LBM scheme, giving a lower bound for the fluid viscosity and limiting the maximum particle lattice speed. For the highest $\mathrm{Re}_p=4$ we used a fluid viscosity $\nu_f=0.02$ and set the Lees-Edwards shift velocity to $u_{\mathrm{LE}}=0.0405$.

For comparison, in Fig. 5 we also plotted shear-thickening measurements obtained by Kromkamp et al. with the ALD method, Couette conditions, and comparable system settings [8]. Our results for the Couette case agree very well with

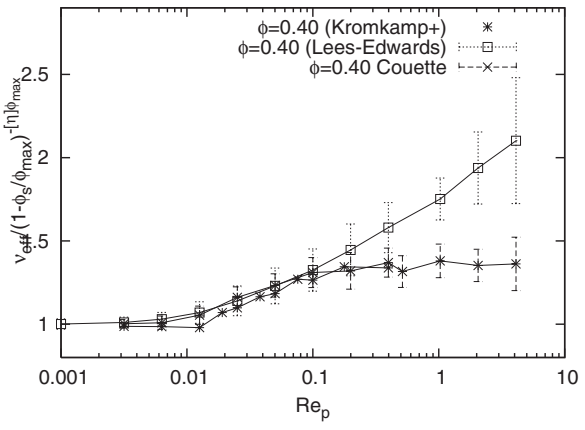

FIG. 5. Apparent viscosity ν_{app} as a function of the particle shear Reynolds number Re_p obtained using the Couette flow scheme and Lees-Edwards boundary conditions. For a comparison also shear-thickening results obtained by applying the ALD method with the Couette flow scheme [8] are shown. Using LEBCs the increase of ν_{app} continues over the range of reachable Re_p.

their data. At about $\mathrm{Re}_p=0.01$ the apparent viscosity begins to increase and levels off at about $\mathrm{Re}_p=0.2$. Also, at the highest Re_p at which we could carry out stable simulation ν_{app} stayed roughly constant. We repeated the experiments using the Lees-Edwards boundary conditions proposed in this work and obtained a behavior that significantly differs from the Couette results for $\mathrm{Re}_p>0.1$. Instead of a saturation behavior ν_{app} shows a continued increase. The profiles in Fig. 3 offer a straightforward explanation for this. Using the Couette conditions we see a slip near the wall for $\mathrm{Re}_p>0.1$ which lowers the velocity gradient and the effective shear rate over the bulk.

A direct relation between the actual bulk shear rate and ν_{app} independent of Re_p could not be found to be clearly visible over the plateau range. This may be caused by the different characters of momentum exchange events for different slip velocities. At higher slip velocities, particles may collide with much higher momentum exchange and impact on the particle structure in the bulk but, on the other hand, such events are less frequent in that regime.

When LEBCs are used these wall effects are not present and the suspension can be sheared at the actually intended shear rate, enabling unbiased studies of sheared hard-sphere suspensions. The apparent viscosity obtained with LEBCs shows a continued increase of ν_{app} giving rise to the assumption that shear-thickening either levels off at higher Re_p or that there is a crossover to jamming behavior. There the shear rate is so high that the suspending role of the fluid becomes negligible and particles collide and jam as in a granular medium.

Using this implementation of LEBCs, we could also start extended studies on cluster formation, investigating the growth of typical structures in sheared suspensions. Results will be presented in a forthcoming work. Concerning the present work, we only took care that particle cluster size did not exceed the system size to prevent percolation of particle clusters which would lead to a jammed suspension in a Lees-Edwards system.

For an estimation of the increase in computational effort due to the proposed implementation of LEBCs against a standard Couette flow simulation for systems as used in Sec. IV C we measured the ratio between the run times of both to be 1.06. The additional effort of 6% is still much less than the approximately 30% of the system height at the highest shear rate that cannot be used for measurements due to the bias by the wall. Increase in the distance between the walls to correct for this, as well as increase in the wall speed to maintain the same shear rate in a Couette flow simulation, would lead to a Mach number that is approximately 30% higher and would therefore lead to a potentially higher error of the LB method and to the onset of instabilities. Furthermore, LEBCs do allow for simulations of systems where the typical correlation length (e.g., particle cluster size) would exceed the unbiased bulk width in a Couette flow simulation.

As a final remark, although only of technical importance, we observe that, using LEBCs, the global momentum is not exactly conserved due to numerical inaccuracies of lattice Boltzmann schemes and the absence of solid obstacles which would define a preferred reference frame. We could improve the conservation by a correction of fluid and particle velocities equivalent to a Galilean transform of the whole system, without affecting the physics.

V. SUMMARY

We developed Lees-Edwards boundary conditions for lattice Boltzmann suspension flows, combining the method proposed for fluid-only systems in [30] with an accurate treatment of the solid particles. The approach has been validated in a benchmark (a single particle crossing a LE boundary) showing that it yields consistent particle dynamics. Then, comparing simulations of suspensions, we could demonstrate that known drawbacks of the Couette scheme (e.g., results biased by the existence of walls) can be removed by applying a LEBC approach. Finally, in a typical application, we used LEBCs to investigate the shear thickening of hard-sphere suspensions. Instead of a saturation of $\nu_{\mathrm{app}}(\mathrm{Re}_p)$ (which can again be related to finite-size effects), we obtained a prolonged thickening behavior.

From the presented test cases, we conclude that the proposed algorithm realizes consistent Lees-Edwards boundary conditions for lattice Boltzmann systems, offering a useful approach to further studies of the pure bulk suspension properties in a quasi-infinite sheared flow.

ACKNOWLEDGMENTS

This research is supported by the European Commission, through the COAST project [35] (EU-FP6-IST-FET Contract No. 033664).

[1] H. A. Barnes, J. Rheol. **33**, 329 (1989).
[2] J. J. Stickel and R. L. Powell, Annu. Rev. Fluid Mech. **37**, 129 (2005).
[3] D. R. Foss and J. F. Brady, J. Fluid Mech. **407**, 167 (2000).
[4] A. W. Lees and S. F. Edwards, J. Phys. A **5**, 1921 (1972).
[5] P. J. A. Hartman Kok, S. G. Kazarian, C. J. Lawrence, and B. J. Briscoe, J. Rheol. **46**, 481 (2002).
[6] S. A. Gulmus and U. Yilmazer, J. Appl. Polym. Sci. **98**, 439 (2005).
[7] J. Hyväluoma, P. Raiskinmäki, A. Koponen, M. Kataja, and J. Timonen, J. Stat. Phys. **121**, 149 (2005).
[8] J. Kromkamp, D. T. M. van den Ende, D. Kandhai, R. G. M. van der Sman, and R. M. Boom, J. Fluid Mech. **529**, 253 (2005).
[9] W. R. Hwang and M. A. Hulsen, J. Non-Newtonian Fluid Mech. **136**, 167 (2006).
[10] S. V. Lishchuk, I. Halliday, and C. M. Care, Phys. Rev. E **74**, 017701 (2006).
[11] R. M. Macmeccan, J. R. Clausen, G. P. Neitzel, and C. K. Aidun, J. Fluid Mech. **618**, 13 (2009).

[12] A. J. C. Ladd, J. Fluid Mech. **271**, 285 (1994).
[13] A. J. C. Ladd, J. Fluid Mech. **271**, 311 (1994).
[14] C. Aidun and Y. Lu, J. Stat. Phys. **81**, 49 (1995).
[15] E.-J. Ding and C. K. Aidun, J. Stat. Phys. **112**, 685 (2003).
[16] C. K. Aidun, Y. Lu, and Ding, J. Fluid Mech. **373**, 287 (1998).
[17] E. Lorenz, A. Caiazzo, and A. G. Hoekstra, Phys. Rev. E **79**, 036705 (2009).
[18] S. Succi, *The Lattice-Boltzmann Equation* (Oxford University Press, Oxford, 2001).
[19] S. Chen and G. D. Doolen, Annu. Rev. Fluid Mech. **30**, 329 (1998).
[20] I. Ginzburg, Adv. Water Resour. **28**, 1171 (2005).
[21] Y. H. Qian, D. D'Humières, and P. Lallemand, Europhys. Lett. **17**, 479 (1992).
[22] U. Frisch, B. Hasslacher, and Y. Pomeau, Phys. Rev. Lett. **56**, 1505 (1986).
[23] R. Verberg and A. J. C. Ladd, Phys. Rev. Lett. **84**, 2148 (2000).
[24] M. Bouzidi, M. Firdaouss, and P. Lallemand, Phys. Fluids **13**, 3452 (2001).
[25] Y. Sui, Y.-T. Chew, P. Roy, and H.-T. Low, Int. J. Numer. Methods Fluids **53**, 1727 (2007).
[26] A. Caiazzo and M. Junk, Comput. Math. Appl. **55**, 1415 (2008).
[27] R. M. Macmeccan, Ph.D. thesis, Georgia Institute of Technology, 2007.
[28] N. Q. Nguyen and A. J. C. Ladd, Phys. Rev. E **66**, 046708 (2002).
[29] A. Caiazzo, Ph.D. thesis, Scuola Normale Superiore, Pisa (Italy) and Technische Universität Kaiserslautern (Germany), 2007.
[30] A. J. Wagner and I. Pagonabarraga, J. Stat. Phys. **107**, 521 (2002).
[31] P. Raiskinmäki, A. Shakib-Manesh, A. Jäsberg, A. Koponen, J. Merikoski, and J. Timonen, J. Stat. Phys. **107**, 143 (2002).
[32] A. Komnik, J. Harting, and H. J. Herrmann, J. Stat. Mech.: Theory Exp. (2004) P12003.
[33] G. P. Krishnan and D. T. Leighton, Phys. Fluids **7**, 2538 (1995).
[34] I. M. Krieger and T. J. Dougherty, Trans. Soc. Rheol. **3**, 137 (1959).
[35] www.complex-automata.org